Design and Fabrication of a Novel Quadruple-Band Monopole Antenna Using a U-DGS and Open-Loop-Ring Resonators

Ahmed Boutejdar[1], Mouloud Challal[2], Faiza Mouhouche[2], Kahina Djafri[2], Saad Dosse Bennani[3]

[1]Institute of Electrical Engineering, German Research Foundation, (DFG), Bonn-Braunschweig, Germany
[2]University M'Hamed Bougara of Boumerdes, Institute of Electrical and Electronic Engineering, Signals and Systems Laboratory, Department of Electronics, 35 000 Boumerdes, Algeria.
[3]University Sidi Mohamed Ben Abdellah, Faculty of Sciences and Technics, Fez, Morocco Laboratory of Renewable Energy and Smart Systems
[1]corresponding author, E-mail: boutejdar69@gmail.com

Abstract

In this Article, a novel quadruple-band microstrip patch antenna is proposed for the systems operating at quad-band applications. The antenna structure is composed of modified rectangular patch antenna with a U-shaped defected ground structure (DGS) unit and two parasitic elements (open-loop-ring resonators) to serve as a coupling-bridge. The proposed antenna with a total size of 31×33 mm^2 is fabricated and tested. The measured result indicates that the designed antenna has impedance bandwidths for 10 dB return loss reach about 180 MHz (4.4–4.58 GHz), 200 MHz (5.4–5.6 GHz), 1100 MHz (7.2–8.3 GHz), and 700 MHz (9.6–10.3 GHz), which meet the requirements of the wireless local area network (WLAN), worldwide interoperability for microwave access (WiMAX), C and X bands applications. Good agreement is obtained between measurement and simulation results.

1. Introduction

In modern wireless communication systems, the requirement of multi-band antenna has played an important role for wireless services. Microstrip patch antenna is an attractive candidate to be used as multi-band antennas due to its low physical profile, easy fabrication and low cost. Many patch antennas have been recently reported in the literature to cover such applications, but most of them are single-band, dual-band and tri-bands [1-3] and cover only the wireless local area network (WLAN) and the worldwide interoperability for microwave access (WiMAX) applications. In [4,5], the antenna produced four bands at 4.64, 5.04, 5.62 and 6.22 GHz. In addition, the antenna in [6-18] can generate four bands at 2.8, 4, 5.4 and 6.2 GHz to cover WLAN/WiMAX. However, none of these antennas can satisfy the C and X bands for mobile and satellite applications.

In this article, a microstrip antenna based on modified rectangular patch antenna with a U-shaped defected ground structure (DGS) unit and two parasitic elements (open-loop-ring resonators) to control surface current distribution on the patch antenna to achieve quad-band operation is proposed.

The antenna prototype is fabricated and measured using Rohde & Schwarz R&S®ZNB vector network analyzer (VNA) operating in the 100 KHz – 20 GHz frequency band. The proposed antenna produces four operating frequencies at 4.5, 5.5, 7.54 and 10 GHz which covers systems operating at WLAN, WiMAX, C and X bands applications.

2. The influence of open loop resonators on radiation characteristics

An investigation of the PE1 and PE2 positions is conducted to find out and to be able to control the effect of placing these parasitic elements on the antenna return loss. Fig. 1 and Fig. 2 display, respectively, the PE1 and PE2 positions with the patch and the simulated return losses for various PE1 and PE2 positions. As the Fig. 2 depicts, different positions, in the closeness of the patch, are considered to be as follows: 0.2 mm, 0.4 mm and 0.6 mm for x-coordinates and, 0 mm, 5 mm and 7 mm for y-coordinates. As Fig. 5 shows, a significant decrease in return loss, especially at 5.5 GHz, compared to the ant4 results, is observed. Moreover, the 4th resonant frequency is shifted down, from 10 GHz to 9.3 GHz. Presence of an additional resonant frequency at around 12 GHz is also noticed. Consequently, the parasitic elements positions affect, considerably, the resonant frequencies.

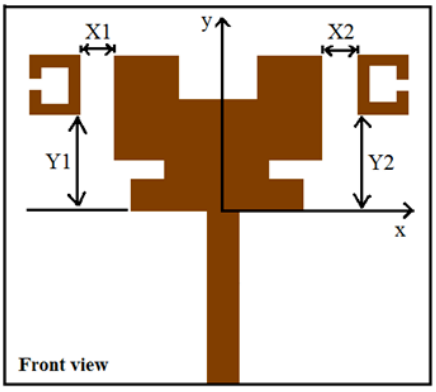

Figure 1. PE1 and PE2 positions with the radiating patch

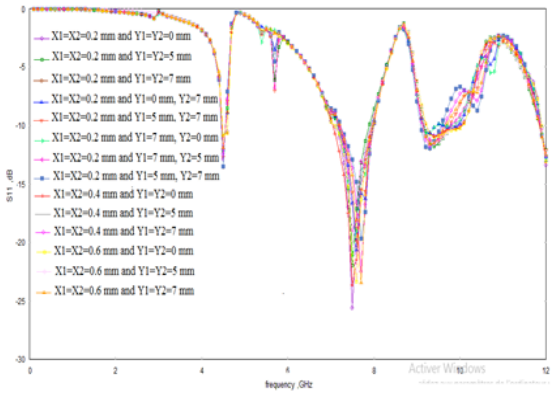

Figure 2. Simulated return loss, S_{11} for various PE1 and PE2 positions.

With other word: a close tunability can be achieved basing on the coupling distance between the open loop resonators and feed line. The disadvantage in this case is that the closed coupling with the radiated patch may affect negatively the performance of the desired antenna in order to deviate from this problem, while keeping the same antenna results. For this aim, the new positions of the open loop resonators, with the idea to be far from the radiating area, are selected (chapter 3).

3. The alternative antenna design

The configuration of the proposed microstrip quadruple-band antenna, fed by 50 Ω microstrip feed line, is shown in Fig. 3. The design consists of modified structure of a rectangular patch antenna with a U-shaped DGS unit and two loaded parasitic elements (denoted as PE1 and PE2). The antenna is printed on a 31 × 33 mm^2 flame resistant (FR-4) substrate with a height of 1.6 mm, a relative dielectric constant of 4.3, and a loss tangent of 0.0017.

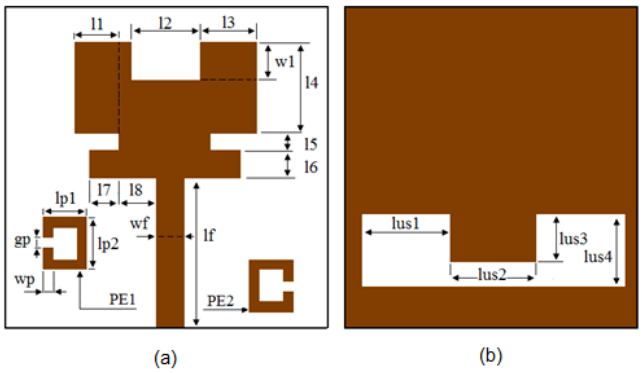

Figure 3. Geometry of the proposed quadruple-band microstrip antenna (a) Front view and, (b) back view.

The design steps to attain the proposed antenna are shown in Fig. 4. The proposed design started with a conventional rectangular patch antenna as shown Fig. 4(a). The modified structure is designed by etching three different parts (U-shaped) from rectangular patch antenna and a U-shaped unit from ground plane as shown Fig. 4(b). Then introducing resonator to act as a parasitic element as shown Fig. 4(c-e). This modified structure generates four resonant modes of operating frequencies. The parameters of the proposed design are illustrated in Table 1.

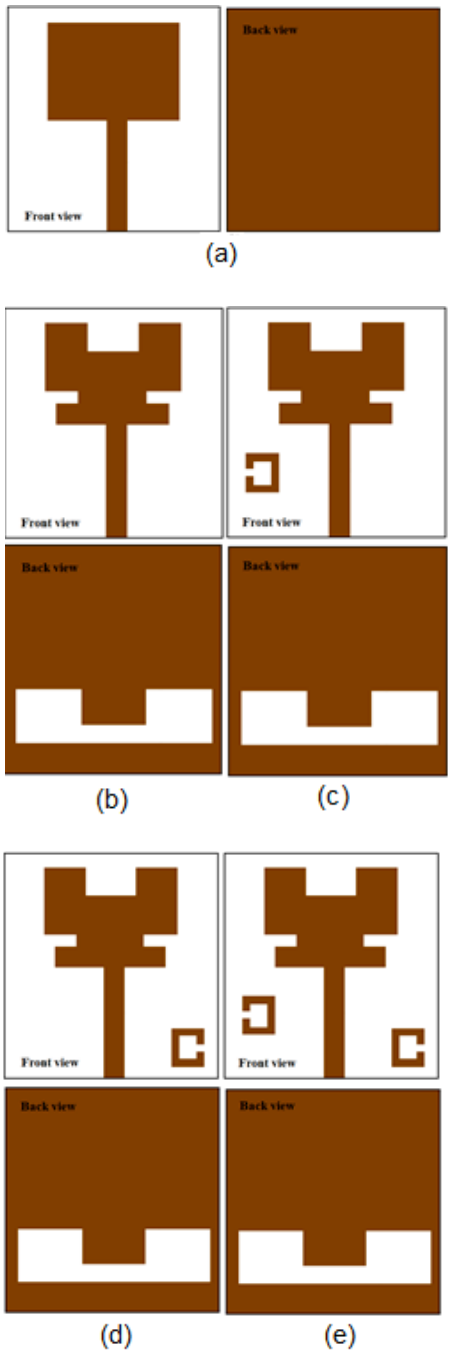

Figure 4. Design steps of proposed quadruple-band microstrip antenna.

Table 1: Dimensions of the proposed quadruple-band microstrip antenna.

Parameters	l1	l2	l3	l4	l5	l6	l7	l8	w1	lf	wf
Dimensions (mm)	50.5	8.89	5.42	10.46	1.97	3.14	3.36	4.24	4.36	17.14	3.15
Parameters	lp1	lp2	wp	gp	lus1	lus2	lus3	lus4			
Dimensions (mm)	4.95	6	1.08	1.22	10	10	5.5	8.21			

4. Simulation results and discussion

The simulation results of antenna with only U-shaped DGS unit (denoted as ant 1), antenna with U-shaped DGS unit and parasitic element 1 (denoted as ant 2), antenna with U-shaped DGS unit and parasitic element 2 (denoted as ant 3) and antenna with both U-shaped DGS unit and the two parasitic elements (denoted as ant 4) are depicted in Fig. 5. The simulated results of ant 1 indicate that the designed antenna achieves quadruple-band operation with resonant frequencies at around 4.5, 5.5, 7.54 and 10 GHz. By adding PE1, ant 2, the second, the third and the fourth resonant frequencies are slightly shifted towards lower frequencies where the second one is more matched. By placing PE2, ant 3, a notched band at the second resonant frequency, 5.5 GHz, is produced and a tri-band operation at about 4.5, 7.50 and 9.5 GHz is achieved. Since the antenna aimed to operate at four distinct resonant frequencies to covers the WLAN, WiMAX, C and X operating bands, a combination of a DGS unit with both PE1 and PE2, ant 4, generates a quadruple - band resonant characteristic at about 4.5, 5.5, 7.54 and 10 GHz with good impedance matching.

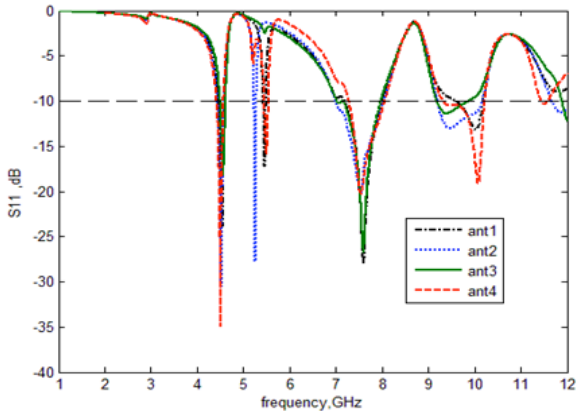

Figure 5. Input reflection coefficients for various antennas involved.

The simulated current distributions at 4.5, 5.5, 7.54 and 10 GHz for the proposed antenna are illustrated in Fig. 6. One can observe that the current distributions are strongly affected by the presence of the DGS unit. The currents are powerfully concentrated in the patch along with feed line and PE1/PE2 at first, third and fourth resonant frequencies. At the second one, the current is mostly concentrated along the PE1 and PE2.

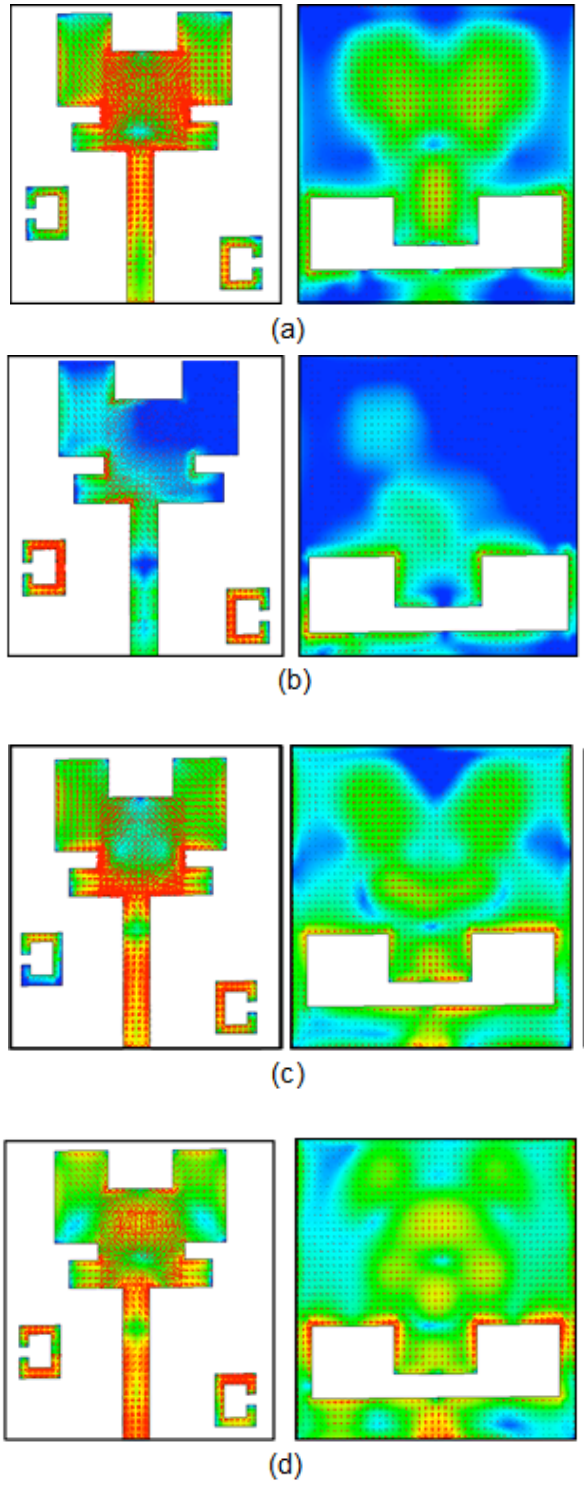

Figure 6. Simulated current distribution of proposed quadruple-band antenna (a) at 4.5 GHz, (b) at 5.5 GHz, (c) at 7.54 GHz and, (d) at 10 GHz.

Fig. 7 illustrates the antenna far zone radiation patterns at the resonant frequencies in both E-plane (φ=0°) and H-plane (φ=90°). In each plane, the radiation pattern is represented in its two components: Co-polar and cross-polar. It can be observed that the 3-dB beam width in both planes at the resonant frequencies are relatively high. Moreover, the maximum directivity in the broadside direction is found to

be 6.05 dBi, 4.64 dBi, 5.58 dBi and 5.49 dBi at resonant frequencies of 4.5 GHz, 5.5 GHz, 7.54 GHz and 10 GHz, respectively. This relatively small level denotes the large broadside nature of the antenna.

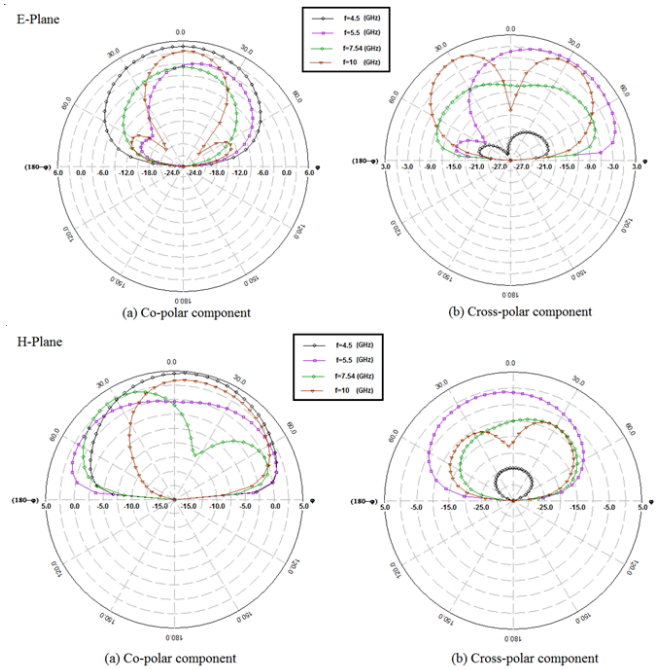

Figure 7. Radiation patterns of the proposed quadruple-band antenna (a) at 4.5 GHz, (b) at 5.5 GHz, (c) at 7.54 GHz and, (d) at 10.07 GHz.

The simulated antenna gain is depicted in Fig. 8. One can observe that the proposed antenna exhibits acceptable gain uniformity with 5.24 dB, 3.98 dB, 5.2 dB and 5.3 dB at 4.5, 5.5, 7.54 and 10 GHz, respectively, which verifies the proposed idea. The radiation efficiency is expected to be small regarding the antenna dimensions and this also can be reflected by a low realized gain within the band.

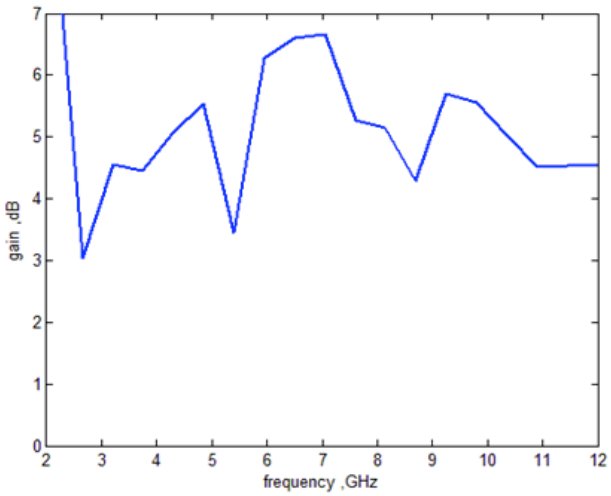

Figure 8. Gain of the proposed antenna.

The gain in [19], given by 2.6 dB, 3.1 dB, 3.8 dB and 6.3 dB at 2.63 GHz, 4.64 GHz, 5.94 GHz and 7.78 GHz, respectively, seems to be smaller than those of our design, except at 7.78 GHz, and this could be realized due to the huge extension of the bandwidth achieved in [19]. Moreover, the pick gain in [20] is approximately same throughout the band except at elevation Y–Z-plane at θ = 90°.

5. Fabrication and measurement results

Based on the parameters illustrated in Fig. 3, the proposed antenna was fabricated and measured using R&S®ZNB VNA. The photograph of the fabricated antenna is shown in Fig. 9. The obtained measurement results are given in Fig. 10 and superimposed to the simulated ones. It can be observed that the measured results are in good agreement with simulated ones. The measured impedance bandwidths for 10 dB return loss reach about 180 MHz (4.4–4.58 GHz), 200 MHz (5.4–5.6 GHz), 1100 MHz (7.2–8.3 GHz), and 700 MHz (9.6–10.3 GHz), which meet the requirements of the WLAN, WiMAX, C and X standards.

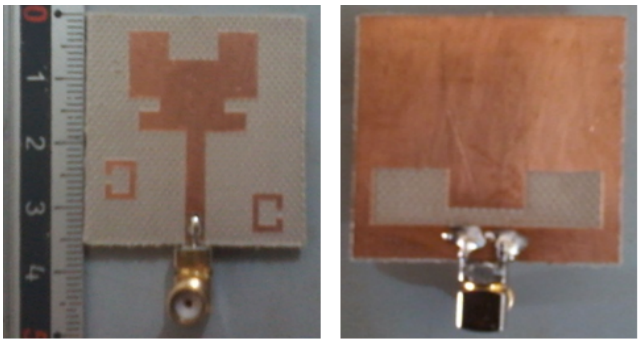

Figure 9. Photograph of fabricated prototype antenna (a) Front view and (b) Back view.

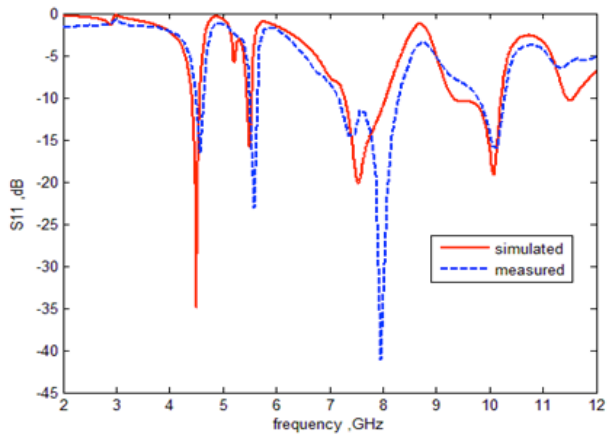

Figure 10. Comparison between simulated and measured of the input reflection coefficients.

The simulated results of the antenna designs depicted in Fig. 4 are tabulated in Table 2. The measured return loss is almost 16, 23, 42, and 16 dB, respectively, for the final design shown in Fig. 4(e), (where f_1, f_2, f_3, f_4) and (RL_1, RL_2, RL_3, RL_4) are respectively resonant frequencies in GHz and corresponding return loss values in dB). In what follow,

the effect of the DGS unit along with the two parasitic elements PE1/PE2 is investigated.

Table 2: Simulated results of the proposed quadruple-band microstrip antenna.

Antenna	f_1	f_2	f_3	f_4	RL_1	RL_2	RL_3	RL_4
ant 1	4.5	5.49	7.56	10	25	17	27	13.5
ant 2	4.5	5.3	7.54	9.5	30	27	20	13.5
ant 3	4.6	-	7.56	9.5	16	-	26	12
ant 4	4.5	5.5	7.54	10	35	15	20	18

6. Conclusions

A novel quadruple-band microstrip patch antenna for WLAN, WiMAX, C and X bands applications has been fabricated and the measurement results have been reported. The measured result have indicated that the proposed antenna has impedance bandwidths for 10 dB return loss attain roughly 180 MHz, 200 MHz, 1100 MHz and 700 MHz which meet the requirements of the WLAN, WiMAX, C and X bands applications. Satisfying experimental results validate the proposed antenna. Good agreement between the simulated and the measured results have been obtained.

Acknowledgements

The author thanks the German Research Foundation (DFG) for financial support. The author thanks M.Sc. Eng. Sonja Boutejdar, Mehdi Boutejdar, Karim Boutjdir, Mohamed Boutejdar for their assistant and help and the responsible of research laboratory, Department of Electronics in University M'Hamed Bougara of Boumerdes, 35000 Boumerdes, Algeria, for their supports.

References

[1] E.K.I. Hamad, N. Mahmoud, Compact Tri-Band Notched Characteristics UWB Antenna for WiMAX, WLAN and X-Band Applications, *Advanced Electromagnetics* 6: 53-58, 2017

[2] L. Kang, H. Wang, X. Shi, Compact ACS-fed monopole antenna with rectangular SRRs for tri-band operation, *Electron. Lett.* 50: 1112–1114, 2014.

[3] A. Kandwal, R. Sharma, S. K. Khah, Dual Band Gap Coupled Antenna Design with DGS for Wireless Communications, *Advanced Electromagnetics* 2: 51-58, 2013.

[4] W.M. Dorsey, A.I. Zaghloul, Dual-band, dual-circularly polarised antenna element, *IET Microwaves, Antennas & Propagation* 7: 283 – 290, 2013.

[5] K. Fertas, H. Kimouche, M. Challal, H. Aksas, R. Aksas, Design and Optimization of a CPW-Fed Tri-band Patch Antenna using Genetic Algorithms, *ACES Journal- Applied Computational Electromagnetics Society Journal* 30: 754– 759, 2015.

[6] V. Singh, B. Mishra, T.P. Narayan, R. Singh, A compact quad-band microstrip antenna for S and C-band applications, *Microw. Opt. Technol. Lett.* 58: 1365– 1369, 2016.

[7] N. Nafiza, B.S. Sreeja, R.C. Devi, S. Radha, Novel axe-shaped circular microstrip quad band antenna, *Microw. Opt. Technol. Lett.* 58: 399–402, 2015.

[8] A. Boutejdar, W. Abd Ellatif, A novel compact UWB monopole antenna with enhanced bandwidth using triangular defected microstrip structure and stepped cut technique, *Microw. Opt. Technol. Lett.* 58: 1514–1519, 2016.

[9] Y. Yu, J. Ni, Z. Xu, Dual-band Dipole Antenna for 2.45 GHz and 5.8 GHz RFID Tag Application, *Advanced Electromagnetics* 4: 31-35, 2015.

[10] M.A. Abdalla, A.A. Ibrahim, A. Boutejdar, Resonator switching techniques for notched ultra-wideband antenna in wireless applications, *IET Microwaves, Antennas & Propagation* 13: 1468–1477, 2015.

[11] A. Ibrahim, M.A. Abdalla, A. Boutejdar, A Printed Compact Band-Notched Antenna Using Octagonal Radiating Patch and Meander Slot Technique for UWB Applications, *Progress In Electromagnetics Research M* 54: 153-162, 2017.

[12] A. Boutejdar, A.A. Ibrahim, E.P. Burte, Novel Microstrip Antenna Aims at UWB Applications, *Microwaves & RF magazine* 7: 8-14, 2015.

[13] A. Boutejdar, A.A. Ibrahim, E.P Burte, A compact multiple band-notched planer antenna with enhanced bandwidth using parasitic strip lumped capacitors and DGS-technique, *TELKOMNIKA Indonesian Journal of Electrical Engineering* 13: 203-208, 2015.

[14] M. Manohar, R.S. Kshetrimayum, A.K. Gogoi, Printed monopole antenna with tapered feed line, feed region and patch for super wideband applications, *IET Microwaves, Antennas Propag*. 8: 39–45, 2014.

[15] M. Krishnan, G. Kannan, Polygon Shaped 3G Mobile Band Antennas for High Tech Military Uniforms, *Advanced Electromagnetics* 5:7-13, 2016.

[16] H. Zhai et al., "A Compact Printed Antenna for Triple-Band WLAN/WiMAX Applications," *IEEE Antennas Wireless Propag. Lett.*, vol. 12, Jan. 2013, pp. 65–68.

[17] W.-C. Liu, C.-M. Wu, and Y. Dai, "Design of Triple-Frequency Microstrip-Fed Monopole Antenna Using Defected Ground Structure," *IEEE Trans. Antennas Propag.*, vol. 59, no. 7, July 2011, pp. 2457–2463.

[18] A. El Alami, S.D. Bennani, A. Slimani, A. Bendali, Comparative study of the radiation patterns of circular patch antenna by using the model approach of the resonant cavity for microwave band RFID reader, *2017 International Conference on Wireless Technologies, Embedded and Intelligent Systems (WITS),* Morocco, 2017.

[19] P.-A. Ambresh, A.-A. Sujata, A.-M. Khan, P.-M. Hadalgi, and P.-V. Hunagund, "Quad Band Rectangular Microstrip Antenna for S and C-Band Applications," *International Journal of Computer and Communication Engineering*, Vol. 3, No. 5, pp. 334-337, Sept. 2014.

[20] J.-P. Thakur, J.-S. Park, B.-J. Jang, and H.-G. Cho, "Small Size Quad Band Microstrip Antenna," *Microwave and Optical Technology Letters*, Vol. 49, No. 5, pp. 997- 1001, May 2007.